

A First-Order Perturbation Analysis of Crack Trapping by Arrays of Obstacles

Huajian Gao

Division of Applied Mechanics,
Stanford University,
Stanford, CA 94305

James R. Rice

Division of Applied Sciences,
Harvard University,
Cambridge, MA 02138

A first-order perturbation analysis is presented for the configuration of an initially straight crack front which is trapped against forward advance by contact with an array of obstacles (i.e., regions of higher fracture toughness than their surroundings). The problem is important to the micromechanics of crack advance in brittle, locally heterogeneous solids. The formulation is based on a linear perturbation result for the stress intensity factor distribution along the front of a half-plane crack when the location of that front differs moderately from a straight line. The trapping solutions for a periodic array of blocking rectangular obstacles are given using an analogy to the plane stress Dugdale/BCS elastic-plastic crack model. For a periodic array of obstacles with a given spacing and size in the direction parallel to the crack front, the obstacle shape may affect the limit load at which the crack breaks through the array. When such effects are examined within the range of validity of the linear perturbation theory, it is found that obstacles whose cross-sections fully envelop a critical reference area give the maximum limit load while others are broken through at lower load levels. We also formulate a numerical procedure using the FFT technique and adopting a "viscoplastic" crack growth model which, in an appropriate limit, simulates crack growth at a critical stress intensity factor. This is applied to show how a crack front begins to surround and penetrate into various arrays of round obstacles (with a toughness ratio of 2) as the applied load is gradually increased. The limitations of the first-order analysis restrict its validity to obstacles only slightly tougher than the surrounding elastic medium. Recently, Fares (1988) analyzed the crack trapping problem by a Boundary Element Method (BEM) with results indicating that the first-order linear analysis is acceptable when the fracture toughness of the obstacles differs by a moderate amount from that of their surroundings (e.g., the toughness ratio can be as large as 2 for circular obstacles spaced by 2 diameters). However, the first-order theory is not only quantitatively inaccurate, but can make qualitatively wrong predictions when applied to very tough obstacles.

Introduction

The micromechanics of crack advance through brittle, locally heterogeneous materials is of fundamental interest. In general, the fracture resistance (local fracture toughness) varies along the front of an advancing macroscopic crack due to microlevel heterogeneities, such as second-phase tough particles which can cause macroscopic toughening of a brittle matrix. This is associated with a process referred to as the "crack trapping," in which the crack front advances nonuniformly and has segments which are trapped, at least

temporarily, by contact with tough particles whose fracture toughness value exceeds the local stress intensity. The problems involved are of three-dimensional character and often lack a theoretical treatment due to mathematical difficulties. Solution procedures based on finite element and boundary element analyses can be devised (see Fares, 1988) and they involve heavy numerical computations. This paper gives a simplified analysis, of limited validity, based on linear perturbation theory for the configuration of an initially straight crack front which is trapped against forward advance by contact with arrays of obstacles. The obstacles are modeled as having the same elastic properties as the rest of the elastic medium, but with slightly higher fracture toughness, so that the material considered here is treated as elastically homogeneous. We assume that the crack grows whenever the local stress intensity factor reaches the local fracture toughness at some point along the crack front. As the applied load increases, the crack front penetrates between and partially into the blocking obstacles and reaches new equilibrium

Contributed by the Applied Mechanics Division of THE AMERICAN SOCIETY OF MECHANICAL ENGINEERS for presentation at the Winter Annual Meeting, San Francisco, Calif., December 10-15, 1989.

Discussion on this paper should be addressed to the Editorial Department, ASME, United Engineering Center, 345 East 47th Street, New York, N.Y. 10017, and will be accepted until two months after final publication of the paper itself in the JOURNAL OF APPLIED MECHANICS. Manuscript received by the ASME Applied Mechanics Division, November 22, 1988; final revision, March 20, 1989.

Paper No. 89-WA/APM-36.

states in which the intensity factor equals the fracture toughness value along the penetrating portions of the crack front. The distribution of stress intensity factors is calculated based on the linear perturbation result, developed earlier in Rice (1985a, 1988), for a half-plane tensile crack with a slightly curved front. The half-plane crack result models finite-sized cracks, assuming the lengths of the cracks are large compared to other parameters such as obstacle spacing along the crack front.

The trapping solutions for a periodic array of rectangular blocking obstacles are obtained using an analogy, following Rice (1988), to the two-dimensional plane stress Dugdale/BCS (for Bilby-Cottrell-Swinden) type of elastic-plastic crack model. The effects of the shape and size of the blocking obstacles on the limit load at which the crack breaks through the obstacles are discussed within the range of validity of the linear perturbation theory, although those concepts can be extended to a broader context.

The limitations of the linear perturbation theory are emphasized here, in that it is accurate only to the first-order in crack front perturbations. This restricts the validity of the present first-order analysis to obstacles only slightly tougher than their elastic surroundings, i.e., the fracture toughness ratio (of the obstacles to surroundings) must be near unity. It will be discussed in the text that when applied to very tough obstacles, the first-order theory is not only quantitatively inaccurate, but can also be qualitatively wrong. Fares (1988) recently performed a BEM (Boundary Element Method) analysis on crack trapping configurations, based on a fundamental solution developed by Rice (1985b), for a prismatic opening dislocation source ahead of a half-plane crack with a straight front. By comparing the BEM results with those obtained by the first-order theory, Fares showed that, for simple cosine wave form perturbations of the crack front, the first-order theory gives quantitatively acceptable results for the stress intensity factor distribution (within 7 percent error) when the wave amplitude is within roughly 0.1 times the wavelength. For the case of periodically emplaced circular obstacles spaced by 2 diameters (Figs. 7, 8), which is analyzed both by Fares (1988) and the present authors, the first-order theory can be applied to obstacles that are up to approximately twice as tough as the surrounding material.

Based on the linear perturbation theory, we formulate a numerical procedure for crack penetration of a periodic array of blocking obstacles by using the Fast Fourier Transform (FFT) technique and adopting a "visco-plastic" crack growth model. In that model, once the stress intensity factor exceeds the local fracture toughness, the rate of the crack growth is taken to be proportional to the difference between them at the same location along the crack front. The crack then continues to grow until the new equilibrium state is reached. By controlling the rate term in such a viscoplastic formulation, the procedure may be made to simulate crack growth with the intensity factor equal, effectively, to the local fracture toughness. We give several examples of applications of the numerical model to show how a crack begins to surround and penetrate into arrays of round obstacles as the applied load is gradually increased.

Formulation of Crack Trapping and Penetration

Following Rice (1988) in formulating the crack trapping problem, we consider a half-plane crack in a linear, isotropic elastic solid. Assume that the crack lies on the plane $y=0$ with a straight tip along $x=a_0$ parallel to the z -axis (Fig. 1(a)), and is subjected to fixed applied tensile loadings which induce mode I tensile stress intensity factor

$$K = K^0[z; a_0] \quad (1)$$

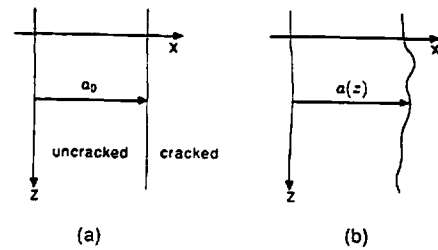


Fig. 1 A half-plane crack in homogeneous, isotropic elastic medium with a (a) straight crack front; (b) slightly-curved crack front

along the crack front. The following linear perturbation result was developed by Rice (1985a) to calculate the distribution of stress intensity factor K along a slightly perturbed crack front, along the arc $x=a(z)$ in the plane $y=0$ (Fig. 1(b))

$$K(z) = K^0[z; a(z)] + (1/2\pi)PV \int_{-\infty}^{+\infty} \frac{K^0[z'; a(z)] [a(z') - a(z)]}{(z' - z)^2} dz' \quad (2)$$

to the first-order accuracy in the deviation of $a(z')$ from constancy; PV denotes principal value. In writing equation (2) for any chosen z , we have chosen a reference straight crack with tip along $x=a(z)$.

We will use these half-plane crack results to model the trapping problems of a finite-sized crack, a_0 now being the crack length in the x -dimension (e.g., half of the length of a tunnel crack). We assume that the real intensity factor distribution along the reference straight crack front varies negligibly with z and also that the representative perturbation wavelength of the actual crack front is much smaller than the overall crack length. Thus the aforementioned half-plane crack result can be used with K^0 regarded as uniform along the crack front and independent of the crack length over the small perturbations to be considered. Note that the representative wavelength of the perturbation of the crack front must be consistent with that of the variation of the nonuniform fracture toughness along the crack front. Using an integration by part in equation (2), one can show that

$$\frac{K(z) - K^0}{K^0} = (1/2\pi)PV \int_{-\infty}^{+\infty} \frac{da(z')/dz'}{z' - z} dz' \quad (3)$$

Let K_c and \hat{K}_c denote the fracture toughness, or the critical K 's, for the obstacle-free material and the obstacles, respectively. Now imagine a crack front that is trapped by obstacles of some given distribution. The crack penetrates between and partially into the obstacles so that we may assume the $K=K_c$ on the portions of the front between the obstacles and $K=\hat{K}_c$ on the portions where the obstacles are being partially penetrated. However, the penetration depth $a(z)$ is unknown in those penetrated zones. Yet, $a(z)$ is known but $K(z)$ is unknown where the crack front just contacts the obstacles. One then needs to solve the singular integral equation (3) for $a(z)$ and $K(z)$ with the values of either $a(z)$ or $K(z)$ given along complementary portions of the z -axis. The special solution to equation (3) with $K(z)=K^0=K_c$ and $a(z)=a_0=\text{const}$, corresponds to the initial state when crack penetration is imminent.

Clearly, equation (3) is strictly valid only if $|da(z)/dz| \ll 1$ over the whole crack front ($-\infty < z < \infty$). This is equivalent to $[K(z) - K^0]/K^0 \ll 1$. Crack penetration into the obstacles starts when the applied K^0 is increased from K_c . Hence, during a penetration process one always has $[K(z) - K^0]/K^0 \leq [\hat{K}_c - K_c]/K_c$ so that the condition $|da(z)/dz| \ll 1$ can be guaranteed by having $[\hat{K}_c - K_c]/K_c \ll 1$. In practical terms it appears that our results are still approximately valid when $[\hat{K}_c - K_c]/K_c$ is near unity.

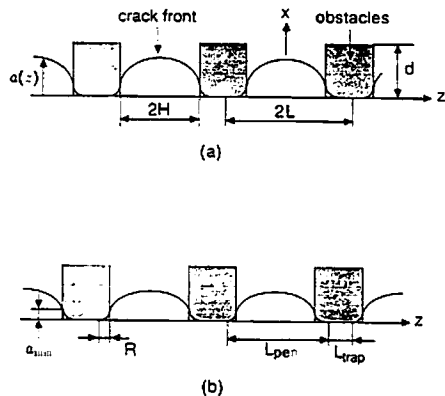


Fig. 2 (a) A crack front trapped by a periodic array of rectangular obstacles and (b) regions L_{trap} , L_{pen} , and R along the trapped crack front

Analogy to Elastic-Plastic Plane Stress Crack Model

Let us consider the two-dimensional plane stress problem in the y, z -plane, with an array of cracks along the z -axis on $y=0$ which can be represented by a continuous distribution of prismatic opening (edge) dislocations. A remotely applied uniform stress $\sigma_{yy} = \sigma^0$ generates an opening gap $\delta = \delta(z)$ (i.e., net y -direction displacement) between $y=0^+$ and $y=0^-$. The stress σ_{yy} along the z -axis, denoted by $\sigma(z)$, is the sum of σ^0 and the effect of a continuous distribution of edge dislocations representing the opening gap between the crack faces. Hence, we write the following,

$$\frac{2[\sigma(z) - \sigma^0]}{E} = \frac{1}{2\pi} pV \int_{-\infty}^{+\infty} \frac{d\delta(z')/dz'}{z' - z} dz' \quad (4)$$

Equation (4) may be rearranged to coincide exactly with (3) provided that one makes the identifications (Rice, 1988)

$$2[\sigma(z) - \sigma^0]/E - [K(z) - K^0]/K^0; \quad \delta(z) - a(z). \quad (5)$$

Thus, the three-dimensional linearized perturbation problem of a crack trapped by, penetrating between, and partially into an array of blocking obstacles has the following two-dimensional plane stress analog: The z -axis is divided into the following two parts, L_{trap} and L_{pen} , analogous to the contact and penetration regions along the crack front (see Fig. 2(b)). Along L_{trap} the plane stress opening gap is prescribed, i.e., as a given distribution of prismatic opening dislocation corresponding to $\delta(z) = a(z)$. Along the portions of L_{pen} between the obstacles, conditions correspond to an array of plane stress cracks with the stress sustained along the crack faces prescribed as $\sigma(z) = \sigma^0 + E(K_c - K^0)/2K^0$. The region denoted as R in Fig. 2(b), as a part of L_{pen} , is analogous to a Dugdale/BCS line plastic zone in plane stress, along which $\sigma(z) = \sigma^0 + E(\hat{K}_c - K^0)/2K^0$. The region L_{trap} reduces, and R increases, with increase of the "applied" stress intensity K^0 , as the crack front gradually penetrates into the obstacles. The size of the zones R must be determined as part of the solution by imposing the condition that $K(z)$ be finite (equal to \hat{K}_c) as the border between L_{trap} and R is approached from within L_{trap} . A special case when $\hat{K}_c \rightarrow \infty$, corresponding to impenetrable obstacles, has the analogy of purely-elastic plane stress cracks without plastic regions.

The plastic flow in the aforementioned analogous two-dimensional plane stress problem, of an array of cracks in an elastic-plastic sheet, is confined to line plastic zones along the z -axis. Thus $\sigma(z) = \hat{\sigma}_c (> \sigma^0)$ along the plastic zones R , where the Dugdale/BCS tensile yield strength $\hat{\sigma}_c$ is identified as $\sigma^0 + E(\hat{K}_c - K^0)/2K^0$. The portions of L_{pen} complementary to R correspond to loaded crack faces on which $\sigma(z) = \sigma_c (< \sigma^0)$ ($\sigma_c = \sigma^0 + E(K_c - K^0)/2K^0$).

Hence, the solutions for the three-dimensional problem of crack trapping by obstacles can be simply extracted from the known two-dimensional Dugdale/BCS plane stress crack model solutions, or from new solutions that can be generated by solving the integral equation or, perhaps, by solving an alternative numerical model of the two-dimensional plane stress problem.

Gradual Penetration of a Periodic Array of Obstacles

Figure 2 shows a periodic array of obstacles with center-to-center spacing of $2L$ and a gap $2H$ between them. The obstacles have flat edges, parallel to the z -axis, and are aligned so that the crack front encounters them simultaneously. Thus they could represent aligned rectangular-shaped obstacles of sufficiently large (see the following) extent d in the x -direction. As remarked, the trapping solution may be developed directly from the analogy to the two-dimensional solution of plane stress Dugdale/BCS model. The Dugdale/BCS model for a periodic crack array has been solved by Bilby and Swinden (1965) and Smith (1966). In particular, the parameters R and a_{min} , characterizing spread of the crack into the obstacles as defined in Fig. 2(b), are given by:

$$R = H \left\{ (1/\epsilon) \arcsin[\sin\epsilon/\sin\mu] - 1 \right\}$$

$$a_{\text{min}} = \frac{2H}{\pi} \frac{\omega \sin\alpha}{\epsilon} \int_{\mu}^{\pi/2} \frac{\cos\phi}{(1 - \sin^2\alpha \sin^2\phi)^{1/2}} \ln \left[\frac{\sin(\phi + \mu)}{\sin(\phi - \mu)} \right] d\phi \quad (6)$$

where

$$\mu = \pi(\hat{K}_c - K^0)/2(\hat{K}_c - K_c), \quad \omega = (\hat{K}_c - K_c)/K^0,$$

$$\epsilon = \pi H/2L, \quad \alpha = \pi(H + R)/2L. \quad (7)$$

These results are meaningful for the range

$$K_c \leq K^0 \leq K_c + f(\hat{K}_c - K_c) \quad (8)$$

where $f = (L - H)/L$ is the line fraction of contact zones. The crack front is predicted, within the linear perturbation formulation, to completely penetrate the obstacles (i.e., L_{trap} shrinks to zero in Fig. 2(b)) at the upper limit. Of course, the linear perturbation procedures themselves are rigorously valid only for K^0 slightly greater than the lower limit K_c . Note that $\mu = \pi/2$ corresponds to the lower limit and $\mu = \epsilon$ to the upper limit.

The upper limit in (8) gives the limit load at which the crack front just breaks through the array of obstacles,

$$K^0 = K_c + f(\hat{K}_c - K_c). \quad (9)$$

This predicts the maximum load that the crack obstacle system can sustain within the range of validity of the linear perturbation theory.

However, the limit load K^0 can be calculated exactly (Rice, 1988) if $K(z)$ is known everywhere along the crack front when the final failure of the crack obstacle system occurs. This would be true if the obstacles are fully penetrated prior to the final failure, so that the local $K(z)$ is everywhere equal to the local toughness. Since it is assumed here that the straight-crack-front value K^0 of equation (1) can be regarded as constant, it is necessary that

$$(K^0)^2 = \langle [K(z)]^2 \rangle \quad (10)$$

be satisfied for any crack front configuration $a(z)$ in Fig. 1(b). Here the brackets denote an average along the entire z -axis. Equation (10) can be proved by considering the energy release in a unit translation of the crack front in the x -direction

without any change of the crack front shape. If no instabilities occur, $K(z)$ is known everywhere at final breakthrough, i.e., $K(z) = K_c$ on regions between the obstacles and $K(z) = \hat{K}_c$ within the obstacles. Hence, equation (10) gives the exact value of the limit load K^0 as

$$K^0 = [K_c^2 + f(\hat{K}_c^2 - K_c^2)]^{1/2}. \quad (11)$$

This agrees with equation (9) to first-order in $(\hat{K}_c - K_c)$ and a table comparing the results over a range of parameters is given by Rice (1988).

However, crack obstacle systems can also fail by mechanisms involving instabilities that occur before the crack front has fully penetrated the blocking obstacles, in which case (11) does not apply. The BEM analysis of Fares (1988) showed that for a crack trapped by sufficiently tough obstacles, there is a maximum local $K(z) = WK_c$ which can be generated at the crack front prior to final instability. When the obstacle toughness \hat{K}_c is more than WK_c , the penetrating crack front segments coalesce with one another and the crack front bypasses the still-intact obstacles. This mechanism of the final instability is completely different from anything explainable within the first-order theory. In fact, the first-order theory predicts that failure always occurs by having the crack front break through the obstacles, and the K^0 at breakthrough increases linearly with the obstacle toughness. The first-order theory also implies that an arbitrarily large local $K(z)$ can be developed where a crack is blocked by a sufficiently tough array of obstacles. Therefore, the first-order theory can be even qualitatively, as well as quantitatively, wrong when applied to tough obstacles.

Hence, W is defined as a critical parameter which sets the upper limit of the obstacle toughness value $\hat{K}_c = WK_c$ for having a breakthrough mechanism as predicted by the first-order theory. In other words, W sets the boundary between the breakthrough mechanism in which case the first-order theory is at least qualitatively correct and the bypass mechanism (coalescence of penetrating crack front segments beyond an unbroken particle) which is completely beyond the scope of the first-order theory. This W can only be determined through more accurate formulations such as the BEM analysis of Fares (1988). Since the maximum local $K(z) = WK_c$, when the penetrating crack front segments start to coalesce unstably, would be determined solely by the configuration of the obstacles, W is dependent on that configuration. For a given center-to-center spacing and obstacle size measured in the z -direction, parallel to the crack front, W is sensitive to the obstacle size d in the x -direction. As a limiting case, W approaches infinity when $d \rightarrow \infty$, as in the case of straight-edge obstacles with semi-infinite extent in the x -direction. The toughness ratio \hat{K}_c/K_c should be significantly smaller than W to get quantitatively acceptable results from linear analysis.

Even if the breakthrough mechanism is guaranteed by having $\hat{K}_c/K_c < W$, there exists another type of instability which leads to final failure before the state of full penetration of the obstacles is attained. In these cases $K(z)$ is not known everywhere at breakthrough (unknown along the unpenetrated portion of the obstacle). For convenience we will refer to such breakthrough processes that become unstable prior to the full penetration of obstacles as "irregular" processes, and others for which $K(z)$ is known everywhere at breakthrough as "regular" processes. In the next section we explore the critical parameters associated with irregular processes within the first-order theory. It will be shown that for rectangular obstacles of given L and H as shown in Fig. 2, a critical length d^L can be defined so that the penetration process is regular if $d > d^L$ and irregular if $d < d^L$.

Therefore, the failure processes of a crack trapped by blocking obstacles fall into three categories. Taking rectangular

obstacles of given L and H as in Fig. 2(a) as a demonstration, there are two critical parameters W , d^L . If the toughness ratio $\hat{K}_c/K_c > W$, the crack will bypass the obstacles without breaking them (category 1). When $\hat{K}_c/K_c < W$, the crack will break the obstacles by penetration. The penetration process will be regular (category 2) if $d < d^L$ and irregular (category 3) if $d > d^L$. The first category involves the mechanism of crack bypassing the unbroken obstacles, which is completely beyond the scope of the first-order theory. We will restrict our attention to the latter categories (2 and 3) of breakthrough mechanism.

For regular processes the obstacles are gradually penetrated by the crack until final breakthrough. The argument leading to equation (11) for rectangular obstacles can be readily extended to arbitrarily-shaped, but symmetric (about the x -direction), blocking obstacles in a periodic array. Let us define $f(x_0)$ as the line fraction of the obstacles on a straight line located at $x = x_0$ parallel to the original crack front. (For rectangular obstacles of Fig. 2, the line fraction $f(x_0)$ is a constant which takes the value of $(L - H)/L$). Equation (11) then gives the exact value of the limit load K^0 , provided that f now represents the maximum line fraction, i.e., $f = \max_{x_0} f(x_0)$. In fact, this is also the upper bound for limit load for irregular penetration processes in the third category. For general, possibly asymmetric blocking obstacles, the limit load for regular processes can still be calculated from (11), but the line fraction f now depends on the crack front profile at final breakthrough. Again considering the energy release in a unit rigid translation of the crack front in the x -direction at the final breakthrough, one easily concludes that $f = S/2L$ where S represents the projection in the z -direction of all the crack front segments within the obstacles in one period. This is even true for multitrow systems of periodic arrays of obstacles (see later examples), in which case the bowing-out crack front will encounter obstacles in different rows.

Assuming $[\hat{K}_c - K_c]/K_c$ is sufficiently small, both regular and irregular crack penetration processes can be studied by first-order perturbation theory. In particular, the irregular processes deserves special attention. We next report a quantitative study on the role of the shape and size of the obstacles in crack penetration processes and discuss the limit load for irregular processes. The case discussed previously, for crack trapping by periodic array of rectangular obstacles with large x -dimension shown in Fig. 2, is important in the following discussions. For convenience we will refer to it as the "model" case.

Irregular Processes in Crack Penetration of an Array of Obstacles

The problem is addressed on the assumption that $[\hat{K}_c - K_c]/K_c$ is within a range suitable for linear perturbation theory. Referring to the model case shown in Fig. 2, we denote the value of a_{\min} at the complete penetration of the obstacles (i.e., $R = L - H$) by a^L , and define the area between the line $x = a^L$ and the crack front within an obstacle by A^L (Fig. 3(a)). Taking the upper limit $\mu = \epsilon = (1 - f)\pi/2$ in equations (6), one obtains

$$\frac{a^L}{L} = \frac{4}{\pi^2} \frac{\hat{K}_c - K_c}{K_c + f(\hat{K}_c - K_c)} \int_0^{f\pi/2} \ln \left[\frac{\sin(f\pi/2 + \phi)}{\sin(f\pi/2 - \phi)} \right] d\phi. \quad (12)$$

Hence, a^L/L is expressed as a function of the line fraction f of the obstacles and the toughness ratio \hat{K}_c/K_c . Now imagine an array of arbitrarily-shaped, but symmetric (about the x -direction), obstacles spaced by $2L$ with a minimum gap of $2H$ in the z -direction. We choose a model case with parameters H , L for reference. If an obstacle can fully contain the area A^L associated with the chosen reference (Fig. 3(b)), then at breakthrough the crack is undergoing exactly the same state as

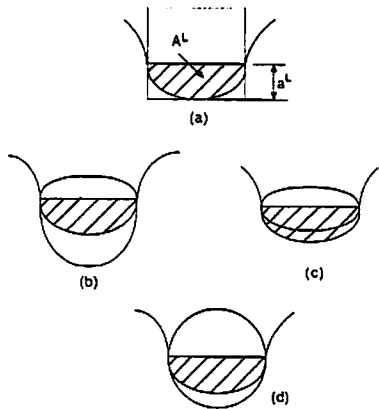


Fig. 3 (a) Area A^L distinguishing between regular and irregular penetration processes; shapes of obstacles that cause (b) regular and (c) irregular processes; (d) round obstacles

the reference model case. Therefore, the penetration process is a regular one so that equation (9) applies to give the limit load based on the maximum line fraction f of the obstacles in the z -direction. For example, it can be proved that $a^L < L - H$ (the proof can be achieved by choosing a variable $u = (L - H)/L$, then forming a function $g(u) = a^L/L - u$ and proving that $g(u)$ is monotonously decreasing from zero over the interval $[0, 1]$). Therefore, the crack penetration of an array of round obstacles with radius equal to $L - H$ is a regular process (Fig. 3(d)), in which case the limit load is predicted by equation (9) for maximum line fraction $f = (L - H)/L$.

However, if the shape of the obstacle can not fully envelop the area A^L of the reference state, but rather is contained (below its maximum width line) fully within A^L (Fig. 3(c)), the full penetration of the obstacle will not be possible at the moment of final breakthrough. That is, an instability will lead to breakthrough prior to the full penetration and the penetration is irregular. Therefore, the area A^L is the critical parameter that distinguishes between the regular and irregular processes. The actual breakthrough loads for irregular processes are smaller than those predicted by equation (9) using the maximum line fraction f .

Usually the calculation of limit loads for irregular processes requires numerical search for the occurrence of instability. However, there are some cases for which direct analysis suffices. For example, consider a periodic array of obstacles with shape shown in Fig. 4(a). Apparently the penetration would be a regular one if the height d of the base portion of the obstacles is greater than a^L , i.e., $d > a^L$. When $d < a^L$, the process is an irregular one if the angle $\psi < \pi/2$. Let us look at a moment at which the crack has penetrated into the obstacle an amount characterized by the parameter p shown in Fig. 4(a). It can be argued that the shown state, if in equilibrium with the imposed load, is the same as another model case with parameter H' defined by $H' = H + p$. It follows from equations (6) that

$$d + p \tan \psi = \frac{4L}{\pi^2} \omega \sin \epsilon \int_{\mu}^{\pi/2} \frac{\cos \phi}{(\sin^2 \mu - \sin^2 \epsilon \sin^2 \phi)^{1/2}} \ln \left[\frac{\sin(\phi + \mu)}{\sin(\phi - \mu)} \right] d\phi \quad (13)$$

where $\epsilon = \pi H' / 2L$ and μ, ω are as defined in equations (7). If we take the derivative of both sides of equation (13), with respect to p , keeping other parameters constant, we can solve for the quantity dK^0/dp for any p . If $dK^0/dp > 0$ the current state is a stable one, in the sense that the load K^0 needs to be increased to increase the penetration p . Instability (failure) occurs when $dK^0/dp \leq 0$ with the critical point reached when the

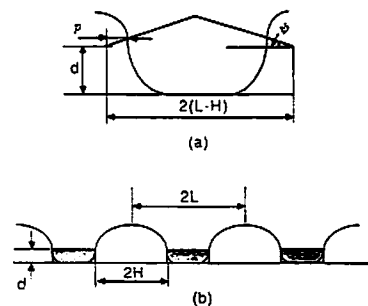


Fig. 4 (a) A special shape of the blocking obstacles; parameter p describing the crack penetration into the obstacles and (b) an example of an irregular penetration process caused by rectangular obstacles

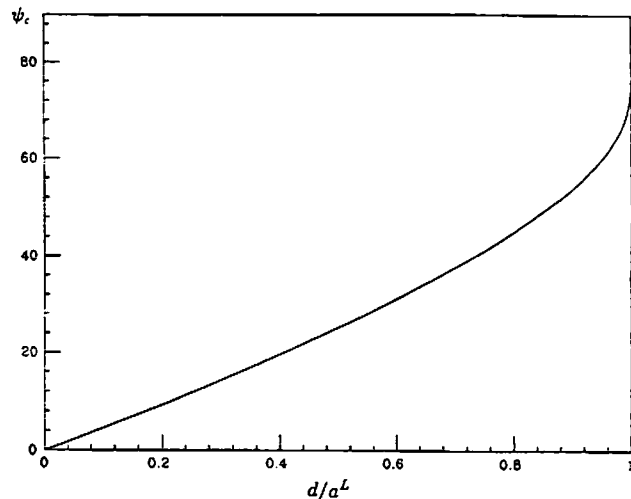


Fig. 5 Critical angle ψ_c for the obstacle shape shown in Fig. 4

equal sign is taken. An important case is $dK^0/dp|_{p=0} = 0$, which determine a critical angle ψ_c below which the instability occurs instantly when $p = 0$. After some algebraic manipulations, it can be shown that

$$\tan \psi_c = \frac{2}{\pi} \omega \int_{\mu}^{\pi/2} \frac{\cos \epsilon \cos \phi \sin^2 \mu}{(\sin^2 \mu - \sin^2 \epsilon \sin^2 \phi)^{3/2}} \ln \left[\frac{\sin(\phi + \mu)}{\sin(\phi - \mu)} \right] d\phi \quad (14)$$

where $\epsilon = \pi H / 2L$ at $p = 0$ and ω, μ are determined further by solving (13) for K_0 using $p = 0$. That is

$$d = \frac{4L}{\pi^2} \omega \sin \epsilon \int_{\mu}^{\pi/2} \frac{\cos \phi}{(\sin^2 \mu - \sin^2 \epsilon \sin^2 \phi)^{1/2}} \ln \left[\frac{\sin(\phi + \mu)}{\sin(\phi - \mu)} \right] d\phi. \quad (15)$$

When the geometrical angle ψ is less than ψ_c , the limit load K^0 at which the crack breaks the obstacles is then determined directly by equation (15). We observe that $\psi_c = \pi/2$ for $\mu = \epsilon$ corresponding to the upper limit in (8), so that at that limit the crack breaks through the obstacles with any ψ , up to $\psi = 90$ deg (corresponding to the model case). As $d \rightarrow 0$, as for a very thin obstacle, $\mu \rightarrow \pi/2$ and $\psi_c \rightarrow 0$. Usually $0 < \psi_c < \pi/2$. The value of ψ_c is plotted in Fig. 5 against d/a^L , the height of the obstacle nondimensionalized by a^L , for $H/L = 0.5$ and $K_c/K_c = 2$. It is shown that ψ_c is increasing in a rather linear fashion with d/a^L until $d/a^L \approx 0.9$, after which a sharp increase toward 90 deg is then observed. A rectangular obstacle with $\psi = 0$ and $d < a^L$ can then be always categorized as $\psi < \psi_c$ (Fig. 4(b)), and the limit load at which a crack breaks through an array of rectangular-shaped obstacles is deter-

mined by the equation (15) when $d < a^L$. Hence, one can define a critical length $d^L (= a^L)$ for rectangular obstacles so that the crack penetration process is regular if $d > d^L$ and irregular if $d < d^L$.

Finally, if $\psi > \psi_c$, instability will occur at some $p > 0$ and a similar critical location can be determined by the condition $dK^0/dp = 0$. We do not present the details of the analysis.

Numerical Formulation of Crack Penetration of Periodic Arrays of Obstacles

Within the range of validity of the linear perturbation theory, we have discussed the problem of crack trapping by a single array of obstacles based on an analogy to the two-dimensional Dugdale/BCS plane stress crack model. The solutions are given for characteristic quantities such as the penetration depths and the limiting K value at which the final breakthrough occurs. In the following we formulate the trapping problem by an alternative, more powerful numerical procedure. The results are compared to those previously derived as well as applied to other cases for which analytical solutions are not known.

General Numerical Formulation. For the general formulation consider that the fracture toughness varies in space so that on the crack plane, $K_c = K_c(x, z)$. The crack will grow at the positions along the crack front where the stress intensity factor exceeds the fracture toughness K_c . We adopt the following "viscoplastic" model for the crack growth

$$\frac{\partial a(z, t)}{\partial t} = \begin{cases} \rho [K(z, t) - K_c(a(z, t), z)] & K < K_c \\ 0 & \text{otherwise} \end{cases} \quad (16)$$

where t is a time parameter in this model and ρ is a coefficient that represents the "viscosity" of the system. By making ρ sufficiently large, or else (as we do) by waiting a sufficiently long time for a new equilibrium configuration of the crack front to be approached after each small increase of load K^0 in a "staircase" load versus time history, we can make (stable) growth occur arbitrarily close to the condition that $K = K_c$ during growth. Mastrojannis et al. (1980) have used a similar (but higher order) criteria in analyzing planar crack growth induced by hydraulic fracturing.

Note that in equation (16), $K = K(z, t)$ is related to $a(z, t)$ by equation (3) at a time t . In principle one can solve the coupled equations (3) and (16) for $K(z, t)$ and $a(z, t)$. Apparently $a(z) = a(z, \infty)$, after step increase to the K^0 of interest, is the final equilibrium crack profile, corresponding to the sort of solution for crack penetration discussed in the previous sections. While it is often impossible to solve the coupled equations analytically, numerical procedures can be designed by discretizing the equation (16) into small time steps, and for each step updating $a(z, t)$ and $K(z, t)$ according to (3). The time step Δt for any given value of ρ can be adjusted to speed up the convergence of the solution. We will apply this procedure to the periodic array of blocking obstacles in the following.

Tunnel Cracks With Periodic Arrays of Obstacles. Consider a tunnel crack lying in a homogeneous, isotropic elastic solid, having length $2a$ along the x -axis, and subjected to a remote tensile stress σ that induces

$$K^0 = K^0[a] = \sigma\sqrt{\pi a} \quad (17)$$

along the crack front. The crack advance is blocked by an array of obstacles. Assuming the half-size of the tunnel crack is initially equal to a_i , crack growth will be imminent once the load σ reaches a point that condition $K^0 = \sigma\sqrt{\pi a_i} = K_c$ is satisfied, where here K_c is the minimum fracture toughness of

the elastic medium along $x = a_i$. With further increase of the load, the crack will grow into a new equilibrium state having a slightly curved front. Now expand $a(z, t)$ and $K(z, t)$ in Fourier series,

$$a(z, t) = \sum_{n=-\infty}^{\infty} A_n e^{in\pi z/L}, \quad K(z, t) = \sum_{n=-\infty}^{\infty} K_n e^{in\pi z/L}, \quad (18)$$

where we recall that $2L$ is the obstacle spacing. Here $A_n = A_{-n}$, $K_n = K_{-n}$ are necessary for $a(z, t)$, $K(z, t)$ to be real valued. Substituting equations (18) into equation (3), and carrying out the principal value integrations, one finds (Rice, 1985a),

$$K_0 = K^0[A_0] = \sigma\sqrt{\pi A_0} \quad \text{and, for } n \neq 0,$$

$$K_n = \left\{ \frac{dK^0[A_0]}{dA_0} - \frac{n\pi}{2L} K^0[A_0] \right\} A_n = \frac{K_0}{2} \left\{ \frac{1}{A_0} - \frac{n\pi}{L} \right\} A_n. \quad (19)$$

Equations (19) replace equation (3) in the case of periodic array of obstacles. Since equation (3) is for a half-plane crack and valid only to the first order in da/dz (or $\partial a(z, t)/\partial z$), equations (19) are only valid when L/A_0 , $|A_n|/A_0 \ll 1$.

For a single cosine wave perturbation assume that $A_n = 0$ for $|n| > 1$ so that $a(z) = A_0 + 2A_1 \cos(\pi z/L)$. In this case, it follows from (19) that

$$K(z) = K_0 \left[1 + \left(1 - \frac{\pi A_0}{L} \right) \frac{A_1}{A_0} \cos(\pi z/L) \right]. \quad (20)$$

Fares (1988) has shown that the error of (20), when $A_1/A_0 \ll 1$, is within seven percent for $A_1 = 0.1L$ but can be as large as 20 percent for $A_1 = 0.2L$. It is seen from (20) that $K(z)$ is predicted to be linear with A_1 , and when A_1/L exceeds $1/\pi$, $K(z)$ is predicted to be negative at the most protruding parts of the crack front, e.g., $z = 0$. This is why the first-order theory can be qualitatively wrong when applied to tough obstacles in which case large crack front perturbations might occur. By contrast, the BEM results of Fares (1988) show that $K(z)$ attains the smallest, but always positive, value at the most protruding parts along the crack front.

The fast Fourier transform (FFT) method is used to carry out the expansion and inversion of the Fourier series in equations (18). The numerical procedure of solving for the equilibrium profile $a(z)$ at a given load σ is then formulated as follows: The initial shape function $a(z, 0)$ (e.g., a constant at the start of the procedure) is expanded into a Fourier series by the FFT method, and the coefficients K_n in the second of equations (18) are calculated by equations (19). A FFT inversion (or summation) by equation (18) gives the distribution of $K(z, 0)$. Equation (16) is then used, for a chosen time interval Δt (sufficiently small for numerical convergence) and constant (arbitrary) ρ , to calculate the amount of growth $\Delta a(z, 0)$ for one period $0 < z < 2L$, therefore updating $a(z, \Delta t)$ as $a(z, 0) + \Delta a(z, 0)$. This procedure is repeated to calculate the subsequent growth until the final equilibrium state is achieved in which $a(z, t)$ no longer increases by any substantial amount (e.g., less than $10^{-6}L$), indicating that conditions $K(z) = K_c$, $K(z) = \bar{K}_c$ are satisfied to the accuracy required along the corresponding portions of penetration. Then the applied stress may be increased by another step and the same sequence of steps followed. We have found that this procedure is a rapidly convergent process for properly chosen time steps (scaling inversely with the constant ρ).

In order to compare the numerical solution to the previously derived results, we consider again the model case of crack penetration into a periodic array of semi-infinite obstacles spaced at gaps of $2L$ as shown in Fig. 2. Figure 6 depicts the obstacles (as lightly-shaded regions) with $H = 0.5L$ and the trapped crack front profiles in one period $-1 < z/L < 1$. The initial crack length a_i is assumed to be 10 times L for the solid

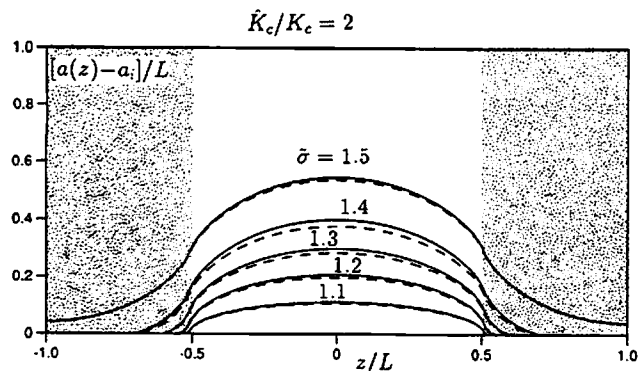


Fig. 6 Crack penetrating a periodic array of straight-edged obstacles aligned in front of a crack with toughness ratio $\hat{K}_c/K_c = 2$. For solid line curves $a_i = 10L$ and for dashed line curves $a_i = 100L$.

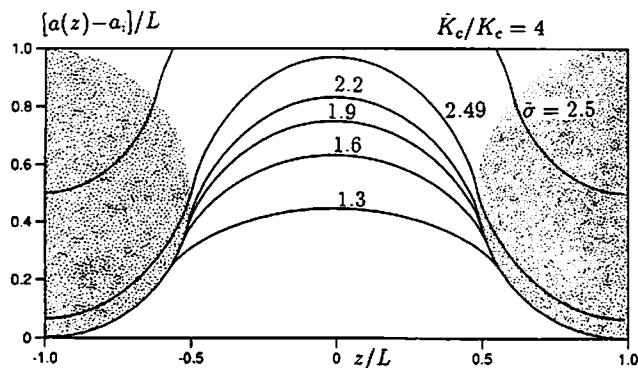


Fig. 7 An array of round obstacles spaced by 2 diameters and the crack trapping profiles when toughness ratio $\hat{K}_c/K_c = 4$ (note that the first-order theory gives qualitatively wrong predictions at the higher $\bar{\sigma}$ values in this case, see text)

line curves. The load σ_i for penetration to start and the initial crack length a_i are related by

$$\sigma_i \sqrt{\pi a_i} = K_c. \quad (21)$$

We define a nondimensional load parameter as $\bar{\sigma} = \sigma/\sigma_i$. The fracture toughness \hat{K}_c of the obstacles is taken as twice the value of K_c . The crack front trapping configurations are shown in solid lines in Fig. 6. The full penetration, which is also the final breakthrough in this special case, occurs when $\bar{\sigma}$ reaches 1.5, as predicted in equation (9). Also shown in Fig. 6 in dashed lines are the corresponding curves when $a_i = 100L$, in which case the half-plane crack is better approximated. We see that the curves for $a_i = 10L$ are very close to those at $a_i = 100L$. The penetration curves also match closely the previously derived a_{\min} and R of equations (6).

Before concluding this section, we further consider a crack penetrating an array of round, circular-shaped obstacles spaced by 2 diameters (Fig. 7). To examine the validity range of the first-order theory, let us first assume a toughness ratio (\hat{K}_c/K_c) of 4. The trapping configurations are shown in Fig. 7 and the final breakthrough occurs at $\bar{\sigma} = 2.5$. Fares (1988) calculated the stress intensity factor distribution corresponding to these first-order-accurate trapping configurations. His results show that only the first profile, corresponding to $\bar{\sigma} = 1.3$, gives the correct $K(z)$ distribution, i.e., $K(z) = K_c$ along the penetrating portion of the crack front. As shown in Fig. 7, the maximum perturbation for the first trapping profile is slightly greater than $0.4L$, which is reasonably consistent with the BEM results on the single cosine wave perturbation shown before. Fares (1988) also pointed out that in this case the maximum local $K(z)$ which can be generated along the crack front is only $3.52K_c$, i.e., $W = 3.52$. The final failure occurs at $\bar{\sigma} = 2.35$, by having the crack front bypass the still-

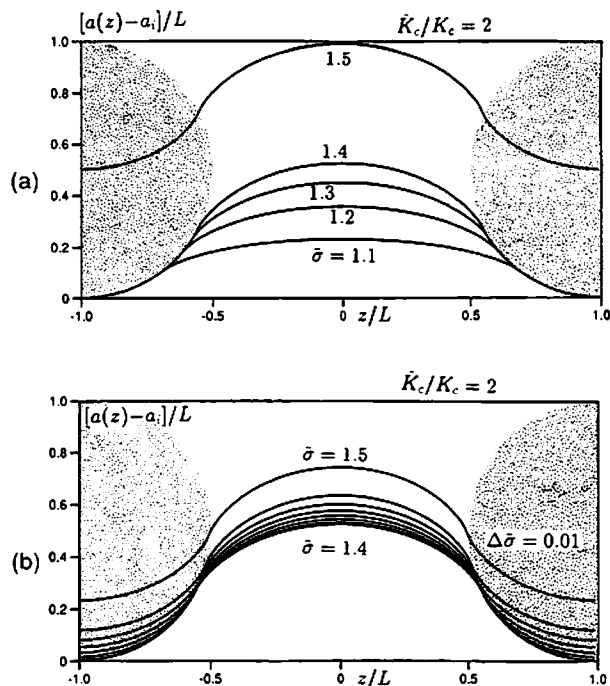


Fig. 8 Crack trapping profiles for round obstacles with toughness ratio $\hat{K}_c/K_c = 2$, when the load σ is increased (a) from 1.1 to 1.5 with a step increment of 0.1 and (b) from 1.4 to 1.5 with a step increment of 0.01

intact obstacles. The first-order-accurate trappings configurations at the higher $\bar{\sigma}$ values in Fig. 7 are, hence, even qualitatively wrong.

This indicates that it is necessary to reduce the toughness ratio substantially in order to apply the first-order theory. The maximum perturbation of the crack front should be kept within a reasonable range. Figure 8(a) depicts the trapping profiles when the toughness ratio is reduced to 2. In this case the maximum perturbation is below $0.6L$ and the linear perturbation theory can be regarded as an acceptable approximation. In Fig. 8(b) a more detailed picture of the crack penetrating the round obstacles is shown as the applied load is gradually increased from 1.4 to 1.5 with a step increment of 0.01. The complete breakthrough of the whole array of obstacles occurs when $\bar{\sigma} = 1.5$. This confirms the previous conclusions that the penetration of round obstacles is a regular process when the toughness ratio is low enough for analysis within the first-order theory. The penetration of the obstacle starts at a load level lower than but close to the final breakthrough load (in our case $\bar{\sigma}_{\text{pen}} = 1.44$). One may see in Fig. 8(a), (b) that the crack initially grows by following closely the outer curvature of the obstacles and starts penetrating the obstacle when $\bar{\sigma} = 1.44$. Shortly after the start of penetration the final breakthrough occurs. This occurs because the circular boundary of the obstacles is close to the bounding curve of A^L . A limiting case is when the shape of the blocking obstacles exactly coincides with the contour of A^L . Then no partial penetration of the obstacles will occur before the final breakthrough.

Some Further Case Studies

Here we give several examples of using the viscoplastic/FFT numerical model to show how a crack starts to penetrate and surround round obstacles, emplaced in the form of multirow periodic arrays, as the applied load is gradually increased. A toughness ratio of two is assumed for each crack obstacle system. The obstacles are shown as lightly-shaded regions in Figs. 9-12.

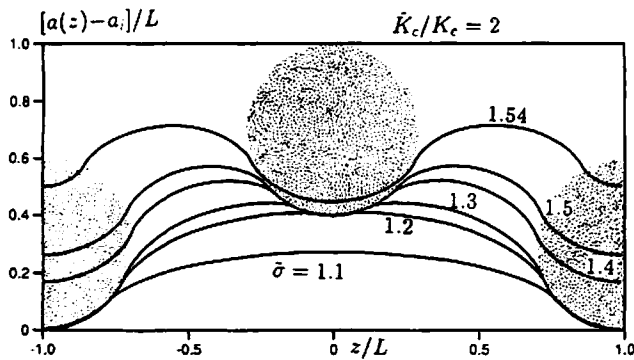


Fig. 9 Case 1: a crack penetrating two rows of periodic arrays of round obstacles with diameter equal to 0.3 times the obstacle spacing

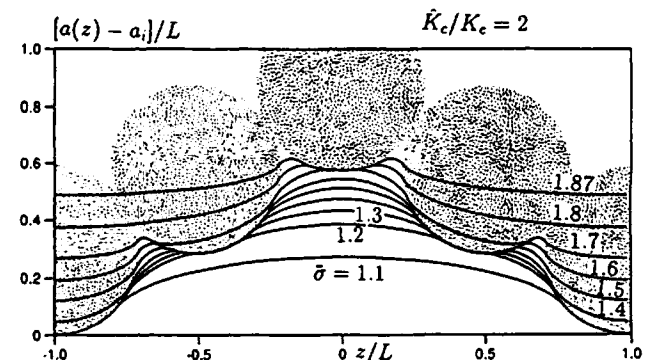


Fig. 11 Case 3: a crack penetrating three rows of periodic arrays of round obstacles with diameter equal to $1/2\sqrt{3}$ times the obstacle spacing

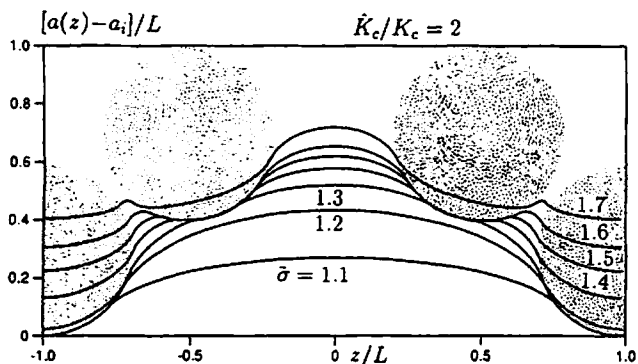


Fig. 10 Case 2: a crack penetrating two rows of periodic arrays of round obstacles with diameter equal to 0.3 times the obstacle spacing

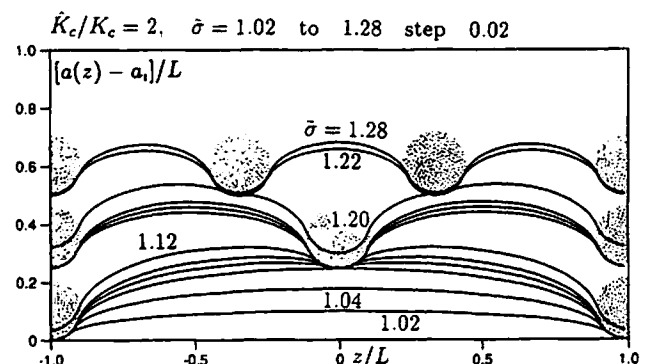


Fig. 12 Case 4: a crack penetrating three rows of periodic arrays of round obstacles with diameter equal to 0.1 times the obstacle spacing

Case 1. Figure 9 shows a two-row periodic array of round obstacles (lightly-shaded circular regions) in one period $-1 < z/L < 1$. The radius of the obstacles is taken as $0.3L$. As can be observed from the resulting crack front trapping configurations, the crack penetration starts by following the circular boundary of the round obstacles in the first row. When load $\bar{\sigma}$ is increased to 1.2, the central part of the penetrating crack front touches the second row of obstacles, and at $\bar{\sigma} = 1.4$, the first row of the obstacles is fully penetrated. The final breakthrough occurs at $\bar{\sigma} = 1.55$.

Case 2. We consider in the second case two rows of round obstacles, still with radius $0.3L$, but with one more obstacle in the second row as shown in Fig. 10. The trapping profiles display more complicated features when the applied load $\bar{\sigma}$ is increased by step increments of 0.1. The first row gets penetrated at $\bar{\sigma} = 1.3$ and the final breakthrough occurs at $\bar{\sigma} = 1.71$.

Case 3. In Fig. 11 three rows of blocking round obstacles are shown, each with radius equal to $L/2\sqrt{3}$. The lines that join the centers of neighboring obstacles are inclined by 30 deg relative to the z -axis (horizontal line). The final breakthrough occurs at $\bar{\sigma} = 1.87$. This obstacle arrangement is interesting, in that a toughening ratio (K_c^0/K_c) of 1.87 is achieved with the area fraction of the obstacles less than 0.5. This occurs because at final breakthrough a large portion of the crack front lies within the obstacle region. Hence, this type of obstacle arrangement is quite efficient in toughening the elastic matrix material. This suggests an interesting problem to find the optimum arrangement for the obstacles at a given volume fraction such that the maximum toughening can be achieved. We leave it as future work to address such issue.

Case 4. Finally, we give a simulation of a crack penetrating smaller particles (with radius taken as $0.1L$) as

shown in Fig. 12. Again, three rows of blocking round obstacles are shown, each row contains one more obstacle such that it is harder to break than the previous row. As the obstacles in the first row have a large spacing, part of the crack front contacts the second row and the interaction effect results in stronger resistance to crack penetration. Such interaction becomes smaller between the second and third row and the final breakthrough occurs at $\bar{\sigma} = 1.30$.

These case studies clearly show that significant toughening of a brittle matrix can be achieved through crack trapping by obstacles (e.g., second-phase particles, inclusions, etc.) by having the obstacles emplaced in a "good arrangement" such that the bowing out crack front encounters the maximum number of obstacles in final breakthrough. In these discussions we have excluded the possibility of having crack bypass tough obstacles (see previous discussions in the text). That mechanism gives rise to unbroken ligaments behind the crack front, which cause an additional toughening effect, referred to as the "bridging effect" in the literature, by reducing the effective crack front stress intensity factor. One expects that, in reality, these mechanisms will have a combined toughening effect on a brittle matrix containing tough second-phase inhomogeneities.

While our considerations here are for tensile (mode I) cracks, the corresponding equations of the first-order perturbation theory are of closely similar form for those loaded in mode II or mode III shear (Gao and Rice, 1986). Thus, to the extent that a shear crack adequately models a tectonic fault, the present considerations may be of interest for faulting in regions of heterogeneous shear toughening.

Acknowledgments

The work reported was supported by subagreement POAVB38639-0 with Harvard University from the University

of California at Santa Barbara, based on ONR contract N00014-86-K-0753, and by the U.S. Geological Survey under grant 14-08-0001-G1367 to Harvard. We are grateful to Dr. Nabil Fares for valuable discussions.

References

- Bilby, B. A., and Swinden, K. H., 1965, "Representation of Plasticity at Notches by Linear Dislocation Arrays," *Proc. Roy. Soc.*, Vol. 285A, pp. 23-33.
- Fares, N., 1988, "Crack Front Trapped by Arrays of Obstacles: Numerical Solutions Based on Surface Integral Representation," *ASME JOURNAL OF APPLIED MECHANICS*, Vol. 56.
- Gao, H., and Rice, J. R., 1986, "Shear Stress Intensity Factors for a Planar Crack With Slightly Curved Front," *ASME JOURNAL OF APPLIED MECHANICS*, Vol. 53, pp. 774-778.
- Mastrojannis, E. N., Keer, L. M., and Mura, T., 1980, "Growth of Planar Cracks Induced by Hydraulic Fracturing," *International Journal of Numerical Methods in Engineering*, Vol. 15, pp. 41-54.
- Rice, J. R., 1988, "Crack Fronts Trapped by Arrays of Obstacles: Solutions Based on Linear Perturbation Theory," *Proceedings of Symposium on Analytical, Numerical and Experimental Aspects of Three-Dimensional Fracture Processes*, ASME-AMD Vol. 91, A. Rosakis, K. RaviChandar, and Y. Rajapakse, eds., pp. 175-184.
- Rice, J. R., 1985a, "First Order Variations in Elastic Fields Due to Variation in Location of a Planar Crack Front," *ASME JOURNAL OF APPLIED MECHANICS*, Vol. 52, pp. 571-579.
- Rice, J. R., 1985b, "Three-Dimensional Elastic Crack Tip Interactions with Transformation Strains and Dislocations," *International Journal of Solids and Structures*, Vol. 21, pp. 781-791.
- Smith, E., 1966, *Proceedings of the 1st International Conference of Fracture*, Vol. 1, T. Yokobori et al., eds., Japanese Society for Strength and Fracture of Materials, Tokyo, pp. 133-152.